Original Paper

Redox equilibria of polyvalent elements in binary $Na_2O \cdot xSiO_2$ melts[1)]

Gordon von der Gönna and Christian Rüssel

Otto-Schott-Institut für Glaschemie, Friedrich-Schiller-Universität, Jena (Germany)

Glass melts with the basic compositions (in mol%) of 15 $Na_2O \cdot 85\ SiO_2$ and $Na_2O \cdot 2\ SiO_2$ were doped with oxides of various polyvalent elements. At temperatures in the range of 800 to 1550 °C, square-wave voltammograms were recorded, which exhibit distinct maxima attributed to respective reduction processes. The following redox steps were observed: Sb^{5+}/Sb^{3+}, Sb^{3+}/Sb^0, As^{5+}/As^{3+}, As^{3+}/As^0, Cu^+/Cu^0, V^{5+}/V^{4+}, V^{4+}/V^{3+}, Cr^{6+}/Cr^{3+}, Cr^{3+}/Cr^{2+}, Fe^{3+}/Fe^{2+} and Ti^{4+}/Ti^{3+}. Peak potentials measured in the $Na_2O \cdot 2\ SiO_2$ glass depended linearly on temperature, while those of the 15 $Na_2O \cdot 85\ SiO_2$ melt were affected by the crystallization of cristobalit at temperatures ≤ 1300 °C. Redox equilibria in the alkali-rich $Na_2O \cdot 2\ SiO_2$ melt were generally shifted to the oxidized state by comparison to those measured in the 15 $Na_2O \cdot 85\ SiO_2$ melt.

Redoxgleichgewichte polyvalenter Elemente in binären $Na_2O \cdot xSiO_2$-Schmelzen

Glasschmelzen mit der Grundzusammensetzung (in Mol-%) 15 $Na_2O \cdot 85\ SiO_2$ und $Na_2O \cdot 2\ SiO_2$ wurden mit Oxiden verschiedener polyvalenter Elemente dotiert. Im Temperaturbereich von 800 bis 1550 °C aufgenommene Square-Wave-Voltammogramme wiesen ausgeprägte Maxima auf, die jeweils Redoxprozessen zugeordnet waren. Es wurden die folgenden Redoxstufen beobachtet: Sb^{5+}/Sb^{3+}, Sb^{3+}/Sb^0, As^{5+}/As^{3+}, As^{3+}/As^0, Cu^+/Cu^0, V^{5+}/V^{4+}, V^{4+}/V^{3+}, Cr^{6+}/Cr^{3+}, Cr^{3+}/Cr^{2+}, Fe^{3+}/Fe^{2+} and Ti^{4+}/Ti^{3+}. Peakpotentiale, die in der $Na_2O \cdot 2\ SiO_2$-Schmelze gemessen wurden, hingen linear von der Temperatur ab, während diejenigen in der 15 $Na_2O \cdot 85\ SiO_2$-Schmelze bei Temperaturen ≤ 1300 °C von der Cristobalitkristallisation beeinflußt wurden. Die Redoxgleichgewichte in der alkalireichen $Na_2O \cdot 2\ SiO_2$-Schmelze waren, im Vergleich zur 15 $Na_2O \cdot 85\ SiO_2$-Schmelze, generell in Richtung des oxidierten Zustands verschoben.

1. Introduction

Numerous studies on redox equilibria in glass melts were reported in the past few years [1 to 15]. The polyvalent ions are, at high temperatures, in equilibrium with the physically dissolved oxygen of the melt.

$$M^{(x+n)+} + \frac{n}{2} O^{2-} \leftrightarrow \frac{n}{4} O_2 + M^{x+} \qquad (1)$$

with: $M^{(x+n)+}$, M^{x+} = polyvalent element in its oxidized and its reduced form; n = number of electrons transferred.

Generally, studies on the thermodynamics of polyvalent elements are either carried out by equilibration experiments [1 to 5] or, however, by electrochemical measurements at high temperatures [6 to 15]. Equilibrating a melt with a gas atmosphere of well-defined oxygen partial pressure is a time-consuming process which requires, depending on the surface/volume ratio of the melt, some hours or days. Subsequently, the melt is quenched and the $[M^{(x+n)+}]/[M^{x+}]$-ratio of the solid glass is determined by physical or chemical methods. The equilibrium constant as defined by equation (2) can directly be determined.

$$K(T) = \frac{[M^{x+}]}{[M^{(x+n)+}]} [O_2]^{n/4} . \qquad (2)$$

The equilibrium constant $K(T)$ depends on temperature and glass composition and is correlated to the standard free enthalpy, the standard enthalpy and the standard entropy of the redox reaction:

$$\Delta G^0 = \Delta H^0 - T \Delta S^0 = - R T \ln (K(T)) . \qquad (3)$$

In contrast to equilibration methods, voltammetric methods are carried out directly in the melt at high temperatures. The current-potential curves recorded exhibit distinct maxima whose potentials in the case of square-wave voltammetry, the most frequently used method, are equal to the standard potential, E^0, of the redox pair. From the standard potentials, standard free enthalpies and equilibrium constants can be calculated which allow a direct comparison with data obtained by equilibration methods.

$$\Delta G^0 = - n F E^0 (T) . \qquad (4)$$

Received 14 February 2000.

[1)] Presented in German at: 73rd Annual Meeting of the German Society of Glass Technology (DGG) in Halle (Germany) on 2 June 1999.

In the past few years, numerous voltammetric studies especially on the thermodynamics of the Fe^{3+}/Fe^{2+} equilibrium have been reported [11 to 15]. These studies were carried out in various melt compositions, such as alkali-lime-silicate, alkali-magnesia-silicate and alkali-lime-alumosilicate melts. The effect of the melt composition upon the Fe^{3+}/Fe^{2+} equilibrium was described by means of empirical equations.

In a few melt compositions, the thermodynamics of various polyvalent elements was studied and electrochemical series of elements were established. Since numerous experiments have to be performed, this was limited to few compositions [9, 10 and 16 to 18]. Hence, the effect of glass composition on the thermodynamics of polyvalent elements is not yet well described and hardly understood.

This paper gives a direct comparison of the thermodynamics of polyvalent elements in two binary soda silicate melts of the basic compositions of $Na_2O \cdot 2\ SiO_2$ and $15\ Na_2O \cdot 85\ SiO_2$.

2. Experimental procedure

The voltammetric experiments were carried out in a resistance-heated furnace ($MoSi_2$). In the middle of the tube, a platinum crucible with approximately 90 g of the melt was located. From the top, three electrodes were inserted into the melt: a platinum wire as the working electrode (diameter: 1 mm), a platinum plate (size around: 2 cm^2) and a zirconia/air probe as reference. All potentials mentioned in this paper are referenced to this electrode. Electronics were self-constructed. The main part, the potentiostat, controlled the potentials between all electrodes in such a manner that the potential between the working and the reference electrode is equal to the present value.

The electrochemical method applied, the square-wave voltammetry, is a fast potentiostatic pulse method whose potential-time dependence is a staircase ramp superimposed by a rectangular wave of comparable high amplitude (100 mV) and short pulse time, τ ($1 \leq \tau \leq 100$ ms) [19 and 20]. The current is measured at the end of every half-wave, then differentiated and drawn against the mean potential. The current-potential curves exhibit distinct maxima attributed to the polyvalent elements present in the melt. Current-potential curves are deconvoluted using a procedure already described in [21].

3. Results

In figure 1, curve 1, a square-wave voltammogram recorded at 1500 °C in a melt doped with 0.25 mol% V_2O_5 is shown. Curve 2 was recorded in the respective melt without any polyvalent element. Curves 3a and 3b present theoretically calculated current-potential curves, while the superposition of curves 2, 3a and 3b is shown

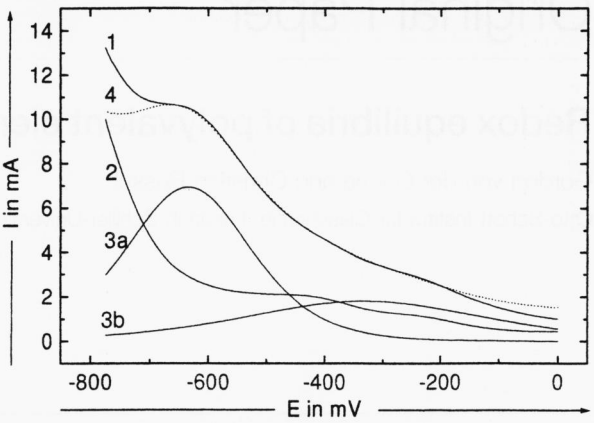

Figure 1. Square-wave voltammogram recorded in a glass melt with the basic composition of $15\ Na_2O \cdot 85\ SiO_2$ doped with 0.25 mol% V_2O_5 at 1500 °C and τ = 10 ms (curve 1); curve 2: recorded in a melt without any polyvalent element, curves 3a and 3b: theoretically calculated square-wave voltammograms, curve 4: curve 2 + curve 3a + curve 3b.

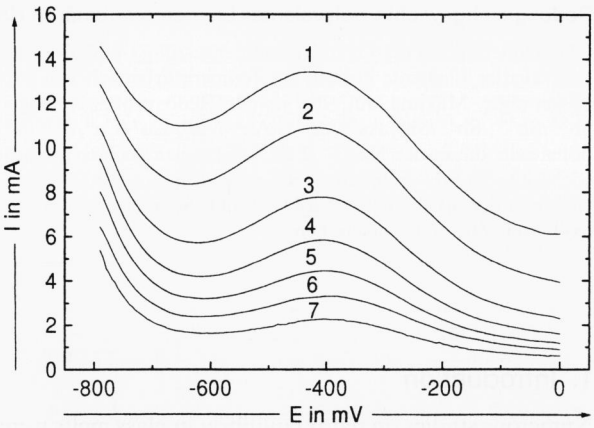

Figure 2. Square-wave voltammograms recorded in a $15\ Na_2O \cdot 85\ SiO_2$ glass melts doped with 0.25 mol% Fe_2O_3 at 1500 °C and at various pulse times; curve 1: τ = 1 ms, curve 2: τ = 2 ms, curve 3: τ = 5 ms, curve 4: τ = 10 ms, curve 5: τ = 20 ms, curve 6: τ = 50 ms, curve 7: τ = 100 ms.

as curve 4. According to [10 and 11], the redox steps attributed to curves 3a and 3b are the reduction of V^{5+} to V^{4+} and of V^{4+} to V^{3+}. They possess peak potentials of −320 and −630 mV, respectively.

$$V^{5+} \xleftrightarrow{e^-} V^{4+} \xleftrightarrow{e^-} V^{3+}. \tag{5}$$

Figure 2 shows square-wave voltammograms recorded in a $15\ Na_2O \cdot 85\ SiO_2$ melt doped with 0.25 mol% Fe_2O_3 at 1500 °C. The curves were recorded at various step times in the range of 1 to 100 ms. They all exhibit a distinct maximum at −410 mV. At potentials less than −650 mV, the currents increase again due to the decomposition of the melt. In this potential range, elemental silicon or platinum silicide is formed at the working electrode. The steady increase in current with decreasing step time is according to theory [19 and 20]. The peak is attributed to the reduction of Fe^{3+} to Fe^{2+}:

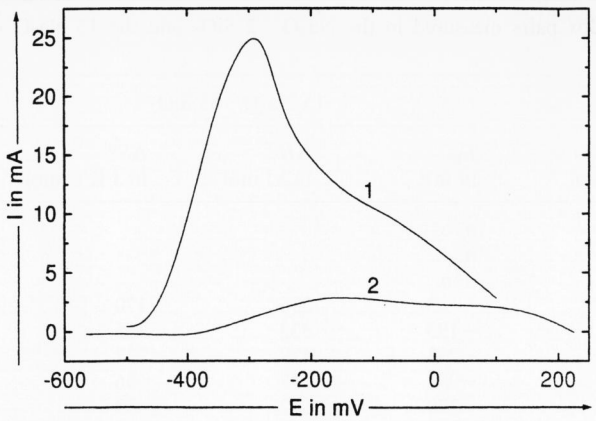

Figure 3. Square-wave voltammograms recorded in glass melts doped with 0.25 mol% As_2O_5 at 1500 °C and τ = 5 ms; curve 1: basic composition $Na_2O \cdot 2\ SiO_2$, curve 2: basic composition $15\ Na_2O \cdot 85\ SiO_2$.

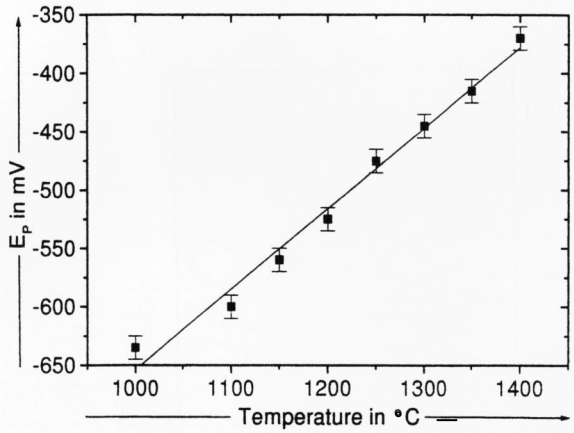

Figure 4. Peak potentials as a function of temperature recorded in a melt with the basic composition of $Na_2O \cdot 2\ SiO_2$ doped with 0.25 mol% CuO.

$$Fe^{3+} \xleftrightarrow{e^-} Fe^{2+}. \tag{6}$$

In figure 3 current-potential curves recorded in arsenic-doped glasses at 1500 °C using a step time of 5 ms are shown. Curve 1 attributed to the $Na_2O \cdot 2\ SiO_2$ composition shows a peak at −290 mV and a shoulder at around −50 mV. By contrast, curve 2 recorded in the $15\ Na_2O \cdot 85\ SiO_2$ melt shows two peaks. The first is observed at +150 and the second at −160 mV. According to [17], the peaks at lower potentials are caused by the reduction of As^{3+} to As^0, while the peak (or the shoulder) at higher potentials is attributed to the reduction of As^{5+} to As^{3+}. The far lower peak currents in curve 2 are caused by lower diffusion coefficients in the melt possessing a much higher viscosity. Figure 3 also shows that the peak potentials are strongly affected by the alkali concentration.

$$As^{5+} \xleftrightarrow{2e^-} As^{3+} \xleftrightarrow{3e^-} As^0. \tag{7}$$

Square-wave voltammograms recorded in melts doped with other polyvalent elements also showed definite

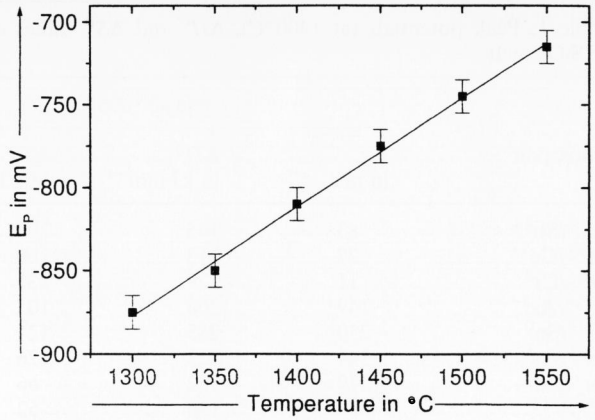

Figure 5. Peak potentials as a function of temperature recorded in a melt with the basic composition of $15\ Na_2O \cdot 85\ SiO_2$ doped with 0.25 mol% TiO_2.

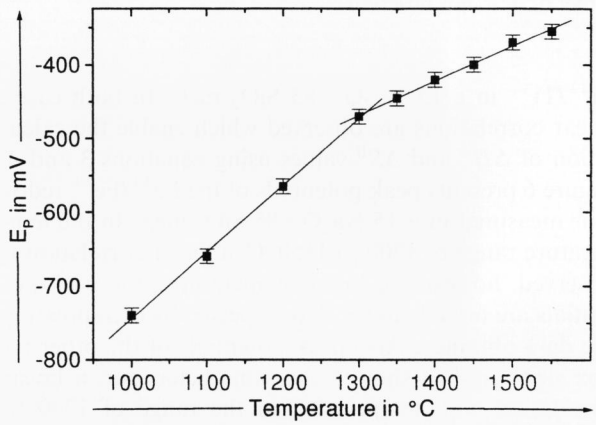

Figure 6. Peak potentials as a function of temperature recorded in a melt with the basic composition of $15\ Na_2O \cdot 85\ SiO_2$ doped with 0.25 mol% Fe_2O_3.

peaks attributed to electrode reactions. Two separate redox steps were also observed in antimony, tin and chromium doped melts.

$$Sb^{5+} \xleftrightarrow{2e^-} Sb^{3+} \xleftrightarrow{3e^-} Sb^0, \tag{8}$$

$$Cr^{6+} \xleftrightarrow{3e^-} Cr^{3+} \xleftrightarrow{e^-} Cr^{2+}. \tag{9}$$

Melts doped with copper or titanium showed only one peak, attributed to the following redox reactions:

$$Cu^+ \xleftrightarrow{e^-} Cu^0, \tag{10}$$

$$Ti^{4+} \xleftrightarrow{e^-} Ti^{3+}. \tag{11}$$

All peak potentials observed depended strongly on temperature. In all cases studied, the peak potentials increased with increasing temperature. Hence all redox equilibria are shifted to the reduced species with increasing temperatures. In figures 4 and 5, this is shown for the redox pairs Cu^+/Cu^0 in a $Na_2O \cdot 2\ SiO_2$ and

Table 1. Peak potentials (at 1400 °C), ΔH^0 and ΔS^0 values of redox pairs measured in the $Na_2O \cdot 2\ SiO_2$ and the $15\ Na_2O \cdot 85\ SiO_2$ melt

redox pair	$Na_2O \cdot 2\ SiO_2$			$15\ Na_2O \cdot 85\ SiO_2$		
	E_P in mV	ΔH^0 in kJ mol^{-1}	ΔS^0 in J K^{-1} mol^{-1}	E_P in mV	ΔH^0 in kJ mol^{-1}	ΔS^0 in J K^{-1} mol^{-1}
Sb^{5+}/Sb^{3+}	83	145	90	n. o.		
Ce^{4+}/Ce^{3+}	77	113	69	n. o.		
Cr^{6+}/Cr^{3+}	11	229	131	n. o.		
As^{5+}/As^{3+}	−149	206	101	3	295	170
Sn^{3+}/Sn^0	−230	285	121	−193	332	155
As^{3+}/As^0	−344	323	126	−233	479	237
Cu^+/Cu^0	−379	152	66	−292	127	56
V^{5+}/V^{4+}	−388	130	52	−370	132	53
Fe^{3+}/Fe^{2+}	−483	126	45	−421	118	43
Cr^{3+}/Cr^{2+}	−704	169	58	−647	165	58
V^{4+}/V^{3+}	−735	151	44	−688	179	63
Ti^{4+}/Ti^{3+}	−857	211	73	−812	190	63

Note: n. o. = not observed.

Ti^{4+}/Ti^{3+} in a $15\ Na_2O \cdot 85\ SiO_2$ melt. In both cases, linear correlations are observed which enable the calculation of ΔH^0 and ΔS^0 values using equations 3 and 4. Figure 6 presents peak potentials of the Fe^{3+}/Fe^{2+} redox pair measured in a $15\ Na_2O \cdot 85\ SiO_2$ melt. In the temperature range of 1300 to 1550 °C, a linear correlation is observed, however, at lower temperatures, the peak potentials are notably lower than expected by extrapolating the data obtained. Also peak potentials of the other redox steps studied showed the same behaviour: a linear correlation with temperature in the range of 1300 to 1550 °C; at further decreasing temperature, peak potentials decreased more than expected. Table 1 summarizes peak potentials measured at 1400 °C in the $Na_2O \cdot 2\ SiO_2$ and the $15\ Na_2O \cdot 85\ SiO_2$ melt (see columns 2 and 5 for the respective redox step). Columns 3 and 4 summarize ΔH^0 and ΔS^0 values of the redox equilibria calculated from E^0 values measured in the $Na_2O \cdot 2\ SiO_2$ melt, respectively. In columns 6 and 7, the ΔH^0 and ΔS^0 values attributed to the $15\ Na_2O \cdot 85\ SiO_2$ melt and temperatures in the range of 1300 to 1550 °C are shown. In figure 7, peak potentials of various polyvalent elements are shown as a function of temperature. Since in all cases linear correlations are obtained, the dependency is illustrated by means of the regression lines.

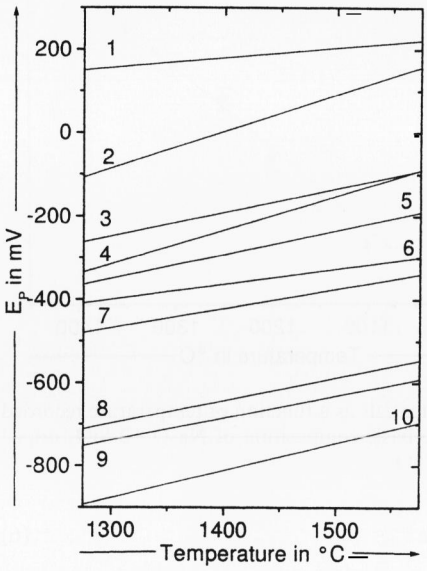

Figure 7. Peak potentials of various polyvalent elements as a function of temperature in melts with the basic composition of $15\ Na_2O \cdot 85\ SiO_2$, illustrated by their regression lines; curve 1: Sb^{5+}/Sb^{3+}, curve 2: As^{5+}/As^{3+}, curve 3: Sb^{3+}/Sb^0, curve 4: As^{3+}/As^0, curve 5: Cu^+/Cu^0, curve 6: V^{5+}/V^{4+}, curve 7: Fe^{3+}/Fe^{2+}, curve 8: Cr^{3+}/Cr^{2+}, curve 9: V^{4+}/V^{3+}, curve 10: Ti^{4+}/Ti^{3+}.

4. Discussion

Peaks observed in the voltammograms can all be explained by assuming redox steps already reported in the literature for melts doped with the respective polyvalent element. All peak potentials measured decrease with decreasing temperature, i.e. all ΔS^0 values calculated are positive. This is in agreement with data in literature, where the same behaviour has already been reported for all polyvalent elements (with the exception of silver [22]) in all glass melts studied up to now. Whereas all peak potentials measured in the $Na_2O \cdot 2\ SiO_2$ melt exhibit a constant slope in the entire temperature range, those attributed to the $15\ Na_2O \cdot 85\ SiO_2$ melt do not show this behaviour. Here, peak potentials depend linearly on temperature in the range of 1300 to 1550 °C, while at lower temperatures, the peak potentials are smaller than expected by extrapolating the high temperature data. Differential thermal analysis of the $15\ Na_2O \cdot 85\ SiO_2$ glass resulted in an exothermic peak at around 1260 °C during cooling the melt from 1450 °C. X-ray diffraction patterns recorded after cooling the $15\ Na_2O \cdot 85\ SiO_2$ melt showed peaks all attributable to cristobalite (Joint Committee on Powder Diffraction Standards, JCPDS nos. 39-1425). Hence, it can be concluded that (i) cristo-

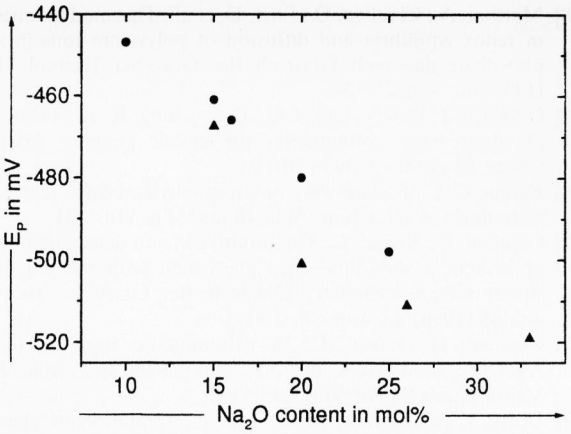

Figure 8. Peak potentials of the Fe^{2+}/Fe^{3+} redox pair as a function of the sodium oxide content for ▲: binary $x\ Na_2O \cdot (100-x)\ SiO_2$, and •: ternary $x Na_2O \cdot 10\ CaO \cdot (90-x)\ SiO_2$ melts.

balite crystallizes at temperatures below 1260 °C, and hence, (ii) sodium oxide is enriched in the melt with decreasing temperature. Therefore, standard potentials measured at temperatures of 1250 °C and below are not attributed to the original melt composition. Since an increase in the alkali content leads to a decrease in the standard potential, the potential-temperature dependence, i.e. the deviation from linearity at temperatures < 1300 °C (see figure 6), can easily be explained by the cristobalite crystallization. At temperatures < 1300 °C, standard potentials are a result of two effects: (i) the shift caused by the decrease in the temperature, and (ii) the shift caused by the enrichment in alkali.

Figure 8 presents standard potentials of the Fe^{2+}/Fe^{3+} redox pair at an arbitrary temperature of 1300 °C as a function of the melt composition. The triangles are attributed to binary $Na_2O \cdot x\ SiO_2$ glasses possessing Na_2O contents of 15, 20, 26 and 33 mol%. As it can be seen, the potentials decrease with increasing Na_2O content. The circles also shown in this figure are data (see [14]) from $x\ Na_2O \cdot 10\ CaO \cdot (90-x)\ SiO_2$ glasses. Here, a linear decrease in the standard potentials upon the Na_2O content is observed within the limits of error. Obviously, the introduction of lime into the glass network leads to an increase in the standard potential. It should be noted that this is in contrast to the basicity concept, because, according to [23 and 24], Na_2O and CaO have almost the same increments to the (calculated) optical basicity. As shown in figure 8, however, CaO has the opposite effect on the Fe^{2+}/Fe^{3+} standard potential as Na_2O.

As shown in table 1, columns 2 and 5 peak potentials measured in the $Na_2O \cdot 2\ SiO_2$ melt are generally lower than those measured in the $15\ Na_2O \cdot 85\ SiO_2$ melt. On the average, the potentials are shifted by around 60 mV in cathodic direction while increasing the Na_2O concentration from 15 to 33.3 mol%. In table 2, redox ratios for various polyvalent elements in the two melt compositions are shown assuming equilibration with air at 1400 °C. Here, the effect of different standard potentials upon the redox ratios is seen. The largest difference (factor 10) was observed in the case of the As^{3+}/As^0 redox pair. It should be noted that this is in agreement with the basicity concept. However, the deviations from that mean shift for the respective polyvalent element is clearly significant. Hence, it can be concluded that specific interactions between the respective polyvalent element and the glass matrix exist and influence the thermodynamics of the attributed redox pair. The electrochemical series of elements in both glasses, however, are similar.

Table 2. Redox ratios calculated from data in table 1 assuming equilibrium with air at 1400 °C

	$[M^{(x+n)+}]/[M^{x+}]$	
redox pair	$Na_2O \cdot 2\ SiO_2$	$15\ Na_2O \cdot 85\ SiO_2$
As^{5+}/As^{3+}	7.9	0.95
Sb^{3+}/Sb^0	$1.2 \cdot 10^2$	56
As^{3+}/As^0	$1.3 \cdot 10^3$	$1.3 \cdot 10^2$
Cu^+/Cu^0	14	6.5
V^{5+}/V^{4+}	15	12
Fe^{3+}/Fe^{2+}	28	19
Cr^{3+}/Cr^{2+}	$1.3 \cdot 10^2$	91
V^{4+}/V^{3+}	$1.7 \cdot 10^2$	$1.2 \cdot 10^2$
Ti^{4+}/Ti^{3+}	$3.9 \cdot 10^3$	$2.8 \cdot 10^2$

5. References

[1] Paul, A.: Effect of thermal stabilization on redox equilibria and colour of glass. J. Non-Cryst. Solids **71** (1985) p. 269–278.

[2] Paul, A.; Douglas, R. W.: Ferrous–ferric equilibrium in binary alkali silicate glasses. Phys. Chem. Glasses **6** (1965) no. 6, p. 207–211.

[3] Lauer, H. V., jr.; Morris, R. V.: Redox equilibria of multivalent ions in silicate glasses. J. Am. Ceram. Soc. **60** (1977) nos. 9–10, p. 443–451.

[4] Schreiber, H. D.; Kozak, S. J.; Merkel, R. C. et al.: Redox equilibria and kinetics of iron in a borosilicate glass-forming melt. J. Non-Cryst. Solids **84** (1986) p. 186–195.

[5] Jeddeloh, G.: The redox equilibrium in silicate melts. Phys. Chem. Glasses **25** (1984) no. 6., p. 163–164.

[6] Takahashi, K.; Miura, Y.: Electrochemical studies on diffusion and redox behavior of various metal ions in some molten glasses. J. Non-Cryst. Solids **38 & 39** (1980) p. 527–532.

[7] Sasahir, A.; Yokokawa, T.: Fe^{3+}/Fe^{2+} redox equilibrium in the molten Na_2O-B_2O_3 system by linear sweep voltammetry. Electrochim. Acta **30** (1985) p. 441–448.

[8] Maric, M.; Brungs, M. P.; Skyllas-Kazacos, M.: Voltammetric and chronopotentiometric reactions of silver ions in molten sodium disilicate glass. Phys. Chem. Glasses **30** (1989) no. 1, p. 12–18.

[9] Rüssel, C.: Voltammetric studies on the redox behaviour of chalcogenides in a soda-lime-silica glass melt. Phys. Chem. Glasses **32** (1991) no. 4, p. 138–141.

[10] Claußen, O.; Rüssel, C.: Thermodynamics of some transition metal ions in a borosilicate glass melt. Phys. Chem. Glasses **38** (1997) no. 5, p. 227–231.

[11] Claußen, O.; Rüssel, C.: Voltammetric study of the thermodynamics of the Fe^{3+}/Fe^{2+} equilibrium and the self diffusivity of iron in glasses with the basic composition $74SiO_2 \cdot (26-x)Na_2O \cdot xCaO$. Phys. Chem. Glasses **39** (1998) no. 4, p. 200–205.

[12] Gerlach, S.; Claußen, O.; Rüssel, C.: Thermodynamics of iron in alkali-magnesia-silica glasses. J. Non-Cryst. Solids **238** (1998) p. 75–82.
[13] Gerlach, S.; Claußen, O.; Rüssel, C.: A voltammetric study on the thermodynamics of the Fe^{3+}/Fe^{2+}-equilibrium in alkali-lime-alumosilicate melts. J. Non-Cryst. Solids **248** (1999) p. 92–98.
[14] Rüssel, C.: Iron oxide-doped alkali-lime-silica-glasses. Pt. 1. EPR investigations. Glastech. Ber. **66** (1993) no. 3, p. 68–75.
[15] Rüssel, C.: EPR and voltammetric studies of iron-containing mixed alkali glasses with the basic composition of $xNa_2O \cdot (16-x)K_2O \cdot 10CaO \cdot 74SiO_2$. Glastech. Ber. Glass Sci. Technol. **70** (1997) no. 1, p. 17–22.
[16] Rüssel, C.; Freude, E.: Voltammetric studies of the redox behaviour of various multivalent ions in soda-lime-silica glass melts. Phys. Chem. Glasses **30** (1989) no. 2, p. 62–68.
[17] Claußen, O.; Rüssel, C.: Thermodynamics of various polyvalent main group elements in a borosilicate glass melt. J. Non-Cryst. Solids **209** (1997) p. 292–298.
[18] Matthai, A.; Claußen, O.; Ehrt, D. et al.: Thermodynamics of redox equilibria and diffusion of polyvalent ions in a phosphate glass melt. Glastech. Ber. Glass Sci. Technol. **71** (1998) no. 2, p. 29–34.
[19] O'Dea, J. J.; Osteryoung, J. G.; Osteryoung, R. A.: Theory of square-wave voltammetry for kinetic systems. Anal. Chem. **53** (1981) p. 695–701.
[20] Barker, G. C.: Square-wave polarography and some related techniques. Anal. Chim. Acta **18** (1958) p. 118–131.
[21] Claußen, O.; Rüssel, C.: Quantitative in-situ determination of iron in a soda-lime-silica glass melt with the aid of square-wave voltammetry. Glastech. Ber. Glass Sci. Technol. **69** (1996) no. 4, p. 95–100.
[22] Claußen, O.; Rüssel, C.: A voltammetric study of the Ag^+/Ag^0 equilibrium in soda-alumina-silicate melts. J. Mol. Liquids **83** (1999) p. 295–302.
[23] Duffy, J. A.; Ingram, M. D.: An interpretation of glass chemistry in terms of the optical basicity concept. J. Non-Cryst. Solids **21** (1976) p. 373–410.
[24] Duffy, J. A.: The refractivity and optical basicity of glass. J. Non-Cryst. Solids **86** (1986) p. 149–160.

0400P002

Address of the authors:

G. von der Gönna, C. Rüssel
Otto-Schott-Institut für Glaschemie
Universität Jena
Fraunhoferstraße 6
D-07743 Jena